Atmos. Meas. Tech. Discuss., 5, 7567–7586, 2012
www.atmos-meas-tech-discuss.net/5/7567/2012/
doi:10.5194/amtd-5-7567-2012

Atmospheric Measurement Techniques Discussions

Measurements of hydrogen cyanide (HCN) and acetylene (C_2H_2) from the Infrared Atmospheric Sounding Interferometer (IASI)

V. Duflot[1], D. Hurtmans[1], L. Clarisse[1], Y. R'honi[1], C. Vigouroux[2], M. De Mazière[2], E. Mahieu[3], C. Servais[3], C. Clerbaux[1,4], and P.-F. Coheur[1]

[1]Spectroscopie de l'Atmosphère, Service de Chimie Quantique et Photophysique, Université Libre de Bruxelles, 50 Av. F. D. Roosevelt, 1050 Brussels, Belgium
[2]Belgian Institute for Space Aeronomy (BIRA-IASB), 3, Av. Circulaire, 1180 Brussels, Belgium
[3]Institut d'Astrophysique et de Géophysique, Université de Liège, 17, Allée du 6 Août, 4000 Liège, Belgium
[4]Université Paris 06; Université Versailles-St. Quentin, CNRS/INSU, LATMOS-IPSL, Paris, France

Received: 5 October 2012 – Accepted: 10 October 2012 – Published: 16 October 2012

Correspondence to: V. Duflot (valentin.duflot@ulb.ac.be), P.-F. Coheur (pfcoheur@ulb.ac.be)

Published by Copernicus Publications on behalf of the European Geosciences Union.

Abstract

Hydrogen cyanide (HCN) and acetylene (C_2H_2) are ubiquitous atmospheric trace gases with medium lifetime, which are frequently used as indicators of combustion sources and as tracers for atmospheric transport and chemistry. Because of their weak infrared absorption, overlapped by the CO_2 Q-branch near 720 cm^{-1}, nadir sounders have up to now failed to measure these gases routinely. Taking into account CO_2 line mixing we provide for the first time extensive measurements of HCN and C_2H_2 total columns at Reunion Island (21° S; 55° E) and Jungfraujoch (46° N; 8° E) in 2009–2010 using observations from the Infrared Atmospheric Sounding Interferometer (IASI). These are compared with local ground-based Fourier Transform InfraRed (FTIR) measurements and we demonstrate that the seasonality is well captured, except for HCN at Jungfraujoch. We also examine a nonspecific biomass burning plume over austral Africa and show that the emission ratios with respect to CO agree with previously reported values.

1 Introduction

Biomass burning is a considerable source of atmospheric trace gases and aerosols at a global scale (Crutzen and Andreae, 1990). Examples include hydrogen cyanide (HCN) and acetylene (or ethyne, C_2H_2). While the primary sources for HCN are attributed to biomass burning, other sources exist, including emissions by fossil fuel combustion and higher plants, bacteria and fungi. The primary sink of HCN is thought to be ocean uptake (Cicerone and Zellner, 1983; Li et al., 2000). However, the magnitudes of these sources and sinks remain uncertain (Li et al., 2009). For C_2H_2, Xiao et al. (2007) evaluated biofuel combustion to be the dominant source, followed by fossil fuel combustion and biomass burning. Reaction with hydroxyl radical (OH) is the main sink for C_2H_2, which may also act as a precursor of secondary organic aerosols (Volkamer et al., 2009).

AMTD
5, 7567–7586, 2012

Aside from their chemical properties, HCN and C_2H_2 are useful tracers of atmospheric transport. Indeed, with a lifetime of 2–4 weeks (C_2H_2) (Logan et al., 1981) to 2–4 months (HCN) (Li et al., 2000), they are effective indicators of how the large-scale distribution of atmospheric pollutants is influenced by long-range transport of biomass and fossil fuel burning. Moreover, the study of the ratio C_2H_2/CO (carbon monoxide) can also help estimate the age of combustion plumes (Xiao et al., 2007).

There are only a limited number of long-term local measurements of HCN and C_2H_2, mainly from ground-based FTIR at selected stations of the Network for the Detection of Atmospheric Composition Change (NDACC, http://www.ndacc.org). Hence, strong uncertainties remain with regard to the magnitude of sources and sinks of HCN and C_2H_2, as well as to their spatial distribution and seasonality in the atmosphere (Li et al., 2009; Parker at al., 2011). Satellite sounders have provided considerable new information in the past years, with measurements from the Atmospheric Chemistry Experiment (ACE-FTS) (Lupu et al., 2009), the Michelson Interferometer for Passive Atmospheric Sounding (MIPAS) (Wiegele et al., 2012) and the Microwave Limb Sounder (MLS) (Pumphrey et al., 2011). These measurements were all made in limb geometry and consequently mostly in the upper troposphere or higher; also the spatial sampling from these instruments is limited. HCN and C_2H_2 have recently been observed using the IASI infrared nadir-looking hyperspectral sounder in a specific biomass burning plume (Clarisse et al., 2011a), as well as in an anthropogenic pollution plume uplifted in the free troposphere (Clarisse et al., 2011b). The purpose of this paper is to show that HCN and C_2H_2 columns can indeed be routinely retrieved from IASI spectra, even in absence of exceptional columns or uplift mechanisms. Having a twice daily global coverage and a 12 km diameter footprint at nadir, the IASI infrared sounder (Clerbaux et al., 2009) aboard the MetOp-A has an obvious potential for providing measurements of these two species globally, and with higher spatial resolution and temporal sampling than what has been obtained up to now. We describe time series and analyze the seasonality of the columns of these two species above two NDACC sites. We also look into the retrieval performances in a typical biomass burning plume.

AMTD
5, 7567–7586, 2012

2 Retrievals

HCN and C_2H_2 are retrieved from IASI radiance spectra with an optimal estimation method (Rodgers, 2000) implemented in the radiative transfer model Atmosphit (Coheur et al., 2005), using absorption bands centered at 713 (ν_2) and 729 (ν_5) cm^{-1}, respectively. Both bands are close to one Q branch of CO_2 centered near 720 cm^{-1}, affected by line-mixing and hence hampering the retrievals of HCN and C_2H_2 when the CO_2 bands cannot be properly simulated. For instance, Clarisse et al. (2011a) had to remove the 715–725 cm^{-1} spectral range from their fits for HCN and C_2H_2 as their forward model did not take into account CO_2 line mixing.

The line mixing effect is due to the increasing overlap of Q lines with increasing pressure, which is such that the contributions of the various transitions are no more additive and the spectrum cannot be simulated by simply summing up the individual line profiles. This is explained theoretically by the fact that intermolecular collisions induce transfer of absorption intensity among the internal levels defining the optical transitions, thus resulting in intensity exchanges between the various spectral components (Hartmann et al., 2008).

The CO_2 line mixing effects are now taken into account in Atmosphit up to 30 km for a wide range of atmospheres by calculating absorption cross sections of CO_2 following the method given in Gamache et al. (2012) and Lamouroux et al. (2012a,b). From 30 km to the top of the atmosphere, where collisions are less frequent, the individual line parameters from the HITRAN spectroscopic database (Rothman et al., 2009) are used. These are also used for all the other species in the line-by-line radiative transfer model.

Figure 1a (red line) shows the difference in the forward model between a spectrum simulated with and without line mixing, along with the spectral signature of HCN (ν_2) and C_2H_2(ν_5) (green and blue lines, respectively). It is clear from the residual spectrum that the spectral fits of HCN and C_2H_2 (and thus the retrievals of their abundance) are

AMTD
5, 7567–7586, 2012

strongly dependent on the accuracy in the simulation of the CO_2 *Q* branch. For this study, line-mixing is included throughout.

The retrievals are performed over the 675 to 775 cm^{-1} spectral range and CO_2, H_2O and O_3 are fitted simultaneously as interfering species. Figure 1b shows the contributions of each of these interfering species assuming background concentrations. For HCN and C_2H_2, we use an ad-hoc covariance matrix with a 100 % variability and we assume the correlation from layer to layer being a 7 km-length exponential decay. These admittedly over simplistic assumptions allow stabilizing the retrieval without too much influence from the a priori information. The a priori profiles used for the forward model and the retrievals with Atmosphit are from the US standard atmospheres when spectra are analyzed over temperate latitudes, and from the standard tropical modeled atmosphere (Anderson et al., 1986) when spectra are analyzed over subtropical latitudes. HCN and C_2H_2 are fitted as profiles, defined by 3 km thick layers from the ground up to 18 km, and by 7 km thick layers from 18 km up to 60 km. However, as the number of degrees of freedom for signal (DOFS) (Rodgers, 2000) is not larger than one for the two species, we analyze in the following only total columns.

3 Comparison with ground based FTIR measurements

We compare in this section HCN and C_2H_2 total columns retrieved from IASI spectra and from ground-based FTIR spectra for the years 2009 and 2010 for two selected NDACC observation sites: Reunion Island (21° S; 55° E) and Jungfraujoch (46° N; 8° E). Note that for both sites and both target species ground-based retrievals are performed in a spectral range between 3250 and 3332 cm^{-1}, which is outside the range covered by IASI. There, the main interfering specie is H_2O and the CO_2 line-mixing effects are less critical and are not accounted for. Detailed description of ground-based FTIR data set, retrieval method and error budget can be found in Vigouroux et al. (2012) for Reunion Island and in Mahieu et al. (2008) and Li et al. (2009) for Jungfraujoch. IASI cloudy spectra were removed from the data set using a 10 % contamination

AMTD
5, 7567–7586, 2012

threshold on the cloud fraction in the pixel, and a posterior filter was also applied to remove poor fits, corresponding to a residual root mean square (RMS) greater than 4×10^{-6} Wm^{-2} msr^{-1}. The resulting mean total retrieval errors on the total columns for HCN and C_2H_2 are 53 % and 47 % at Reunion Island, and 92 % and 77 % at Jungfraujoch. Figure 2 shows the mean total column averaging kernels for IASI and for the ground-based FTIR at each of these sites. We find that the retrieved profiles from IASI spectra are mostly sensitive to the target species abundance in the mid-upper troposphere, with total column averaging kernels peaking at ∼ 9 km for C_2H_2 for both sites, at ∼ 10 km for HCN at Jungfraujoch and at ∼ 14 km for HCN at Reunion Island. We also find that the retrieved profiles from IASI spectra are more sensitive to HCN abundance at Reunion Island than at Jungfraujoch, while the sensitivity to C_2H_2 abundance is quiet similar at both sites. Note that both ground-based instruments have a good sensitivity to HCN abundance in the stratosphere, while IASI total column averaging kernels decrease rapidly to zero above the tropopause.

Figure 3 shows the comparison between the IASI and the ground-based measurements. IASI retrieved total columns were averaged on a daily basis and on a $1^\circ \times 1^\circ$ area around the observation sites. Differences in the a priori profiles used in the retrievals were taken into account following the recommendations in Rodgers (2003). Red circles show ground-based measurements smoothed with respect to IASI averaging kernels, while green dots show unsmoothed ground-based measurements. Note that green dots are not visible when indiscernible from red circles.

One can see that there is an overall agreement between the IASI and the ground-based FTIR measurements considering the error bars. An important result from this study is that IASI seems to capture the seasonality in the two species in most of the cases. This is best seen by looking at the IASI monthly mean retrieved total columns (blue circles and line in Fig. 3). Note that the scattering of the IASI daily mean measurements (black dots) is partially due to the averaging on a $1^\circ \times 1^\circ$ area around the observation sites.

AMTD
5, 7567–7586, 2012

At Reunion Island the HCN and C_2H_2 peaks occur in October–November and are related to the Southern Hemisphere biomass burning season (Vigouroux et al., 2012). We find maxima of around 5×10^{15} mol cm^{-2} for HCN and 3×10^{15} mol cm^{-2} for C_2H_2, with somewhat larger values in 2010 in comparison to 2009. The seasonality and interannual variability matches very well that of the FTIR measurements for HCN (correlation coefficient of 0.80 for the entire daily mean dataset) but with the IASI columns being biased low by 1.72×10^{15} mol cm^{-2} when considering the smoothed ground-based measurements. The results are less satisfactory for C_2H_2 (correlation coefficient of 0.54 for the entire daily mean dataset) due to a much stronger amplitude of the seasonal cycle in the IASI data and possible high bias.

For the Jungfraujoch site, the agreement between IASI and the FTIR retrieved columns is acceptable for C_2H_2 ($R = 0.51$) and the seasonality is similar. The larger columns are indeed retrieved in February by both instruments (maximum of about 3×10^{15} mol cm^{-2} for the IASI monthly mean and the unsmoothed ground-based measurements, and of about 1.8×10^{15} mol cm^{-2} for the smoothed ground-based measurements), caused by the increased C_2H_2 lifetime in winter (Zander et al., 1991). The most important disagreement is found for HCN at the Jungfraujoch site. The correlation coefficient is only 0.15 and the seasonality observed from the ground, showing higher values from spring to autumn due to Northern African and Boreal Asian biomass burning activity (Li et al., 2009), is not captured by IASI, which in fact does not seem to show any clear seasonal variation. Although further analyses would be needed to confirm this, one explanation would be that in a temperate mid-latitude atmosphere, the IASI sensitivity to tropospheric HCN is lower than in a tropical atmosphere (as discussed above and made obvious by the averaging kernels comparison in Fig. 2a). Moreover, stratospheric variations in HCN abundance, which are likely seen in the FTIR time-series (Fig. 2b), are not captured by IASI.

Note that if CO_2 line-mixing effects are not considered in the IASI retrievals, retrieved total columns from IASI spectra do not agree any more with ground-based measurements: for both sites and both target specie, IASI measurements become around one

AMTD
5, 7567–7586, 2012

order of magnitude higher than the ground-based ones. This shows the importance of taking into account CO_2 line-mixing effects in the forward and inverse models of the retrieval method when using absorption bands close to 720 cm^{-1}.

4 Case study: an Austral African biomass burning plume

To further illustrate what can be achieved with the measurements of HCN and C_2H_2 total columns from IASI spectra, this section expounds the study of Clarisse et al. (2011a) for an exceptional fire event, to a regular biomass burning plume. We choose an event that took place over austral Africa and Southern Mozambique Channel on 10 October 2010, which constitutes a typical biomass burning plume within the so-called "river of smoke" yearly exiting Southern Africa toward the Southern Indian Ocean during the Southern Hemisphere biomass burning season (Annegarn et al., 1998; Duflot et al., 2010). To test the validity of the retrieval method for the widest range of situations, the retrievals were performed as exposed in Sect. 2, without any assumption on the altitude of the plume.

Figure 4 shows in red the difference between an observed spectrum on October 10 a.m. at 22.35° S and 33.63° E and the corresponding fitted spectrum with HCN and C_2H_2 excluded. A number of absorption features (most notably at 713 and 729 cm^{-1}) exceed the instrumental noise and can be attributed to HCN and C_2H_2 when compared to the top of the atmosphere contribution of these species (shown in green and blue for HCN and C_2H_2 respectively). In fact, the maximum radiance difference reaches 2×10^{-5} $Wm^{-2}msr^{-1}$ for HCN and C_2H_2, which is an order of magnitude larger than the instrumental noise of 2×10^{-6} $Wm^{-2}msr^{-1}$ in this region (Clerbaux et al., 2009).

Figure 5 shows the total columns (in $mol\,cm^{-2}$) of CO (retrieved in near-real-time from FORLI software, Hurtmans et al., 2012), HCN and C_2H_2, respectively, on 10 October. Note that to produce the distributions, the cloudy spectra were removed from the data set and retrievals with errors greater than 100 % were also excluded. The resulting mean total retrieval errors for HCN and C_2H_2 total columns are 26 % and 68 %. We

AMTD
5, 7567–7586, 2012

see in Fig. 5 that the plume is similar in shape for the 3 species and extends from ~(15° S; 20° E) to ~(35° S; 45° E). It originates very likely from the biomass burning spots detected by the Moderate Resolution Imaging Spectroradiometer (MODIS) in Zambia, Mozambique, Zimbabwe, Botswana and South Africa on 9 and 10 October, as shown by black dots in these figures. Maximum columns in the plume reach 5.9×10^{18} for CO, 4.8×10^{16} for HCN and 3.2×10^{16} mol cm^{-2} for C_2H_2.

Figure 6 shows the correlation plot between CO and HCN (black dots) and C_2H_2 (green circles) total columns. The correlation coefficients are 0.72 and 0.68 for HCN and C_2H_2, respectively, for a total of 1397 retrieval points. This high correlation between the three species, which share biomass burning as an important source, confirms the fire origin of the plume. Given the relatively long lifetimes of the species (several weeks to several months) and the vicinity of the fire sources, the slope of each correlation line gives the emission ratio of the corresponding specie: 0.0092 ± 0.0016 and 0.0055 ± 0.0034 for HCN and C_2H_2, respectively. These values compare very well with the emission ratios with respect to CO derived by Sinha et al. (2003) from aircraft measurements over savanna fires in Southern Africa (0.0085 ± 0.0029 for HCN and 0.0043 ± 0.0013 for C_2H_2).

5 Conclusion and outlooks

We have demonstrated the possibility of retrieving HCN and C_2H_2 columns from IASI radiance spectra in the 720 cm^{-1} region, by properly incorporating CO_2 line mixing in the radiative transfer model. This study shows that the sensitivity of IASI to the two species is mostly in the mid-upper troposphere above 6 km. Total columns have been retrieved for a 2-yr period above Reunion Island and Jungfraujoch, where routine FTIR measurements are available. The comparison between IASI and FTIR retrieved total columns demonstrates the capabilities of IASI to capture the seasonality in HCN and C_2H_2 in most cases (HCN and to lesser extent C_2H_2 at Reunion Island; and C_2H_2 at Jungfraujoch). The absence of seasonality of HCN at Jungfraujoch could

AMTD
5, 7567–7586, 2012

be rationalized by the low sensitivity of IASI to HCN abundance at mid-latitudes. The IASI total columns of HCN (C_2H_2) are shown in this preliminary comparison to be biased low (high) as compared to the smoothed ground-based measurements. A more complete validation study should be carried out to confirm this.

In addition, HCN and C_2H_2 total columns were retrieved within a biomass burning plume over austral Africa and emission ratios with respect to CO were derived from these measurements. The values of 0.0092 ± 0.0016 and 0.0055 ± 0.0034 for HCN and C_2H_2, respectively, agree with values reported in the literature for biomass burning plumes above austral Africa.

In summary, the results presented in this paper have shown for the first time that IASI spectra can be used to establish time series and trends of HCN and C_2H_2 columns at different latitudes, and both for background or highly concentrated (biomass burning plume) environments. Work is ongoing to fully exploit the IASI spatial resolution and temporal sampling, to provide global distributions of these two species.

Acknowledgements. IASI has been developed and built under the responsibility of the Centre National d'Etudes Spatiales (CNES, France). It is flown onboard the Met-Op satellites as part of the EUMETSAT Polar System. The IASI L1 data are received through the EUMETCast near real time data distribution service. Part of the research is supported by EUMETSAT through the O_3SAF project. PFC and LC are respectively Scientific Research Worker and Research Associate at the F.R.S.-FNRS. The research in Belgium was funded by the F.R.S.-FNRS, the Belgian State Federal Office for Scientific, Technical and Cultural Affairs and the European Space Agency (ESA Prodex arrangements C4000103226 and the AGACC-II project). Financial support by the "Actions de Recherche Concertées" (Communauté Française de Belgique) is also acknowledged. The Liège team further acknowledges the Fédération Wallonie-Bruxelles for supporting travel costs to the Jungfraujoch station and wishes to thank the International Foundation High Altitude Research Stations Jungfraujoch and Gornergrat (HFSJG, Bern) for supporting the facilities needed to perform the observations.

AMTD
5, 7567–7586, 2012

References

Anderson, G. P., Clough, S. A., Kneizys, F. X., Chetwynd, J. H., and Shettle, E. P.: AFGL Atmospheric Constituent Profiles (0–120 km), Environmental Research Papers no. 954, AFGL-TR-86-0110, Air Force Geophysics Laboratory, Hanscom AFB, Massachusetts, 1986.

Annegarn, H. J., Otter, L., Swap, R. J., and Scholes, R. J.: Southern Africa's ecosystem in a test-tube: A perspective on the Southern African Regional Science Initiative (SAFARI 2000), S. Afr. J. Sci., 98, 111–113, 2002.

Cicerone, R. J. and Zellner, R.: The atmospheric chemistry of hydrogen cyanide (HCN), J. Geophys. Res., 88, 10689–10696, 1983.

Clarisse, L., R'Honi, Y., Coheur, P.-F., Hurtmans, D., and Clerbaux, C.: Thermal infrared nadir observations of 24 atmospheric gases, Geophys. Res. Lett., 38, L10802, doi:10.1029/2011GL047271, 2011a.

Clarisse, L., Fromm, M., Ngadi, Y., Emmons, L., Clerbaux, C., Hurtmans, D., and Coheur, P.-F.: Intercontinental transport of anthropogenic sulfur dioxide and other pollutants: An infrared remote sensing case study, Geophys. Res. Lett., 38, L19806, doi:10.1029/2011GL048976, 2011b.

Clerbaux, C., Boynard, A., Clarisse, L., George, M., Hadji-Lazaro, J., Herbin, H., Hurtmans, D., Pommier, M., Razavi, A., Turquety, S., Wespes, C., and Coheur, P.-F.: Monitoring of atmospheric composition using the thermal infrared IASI/MetOp sounder, Atmos. Chem. Phys., 9, 6041–6054, doi:10.5194/acp-9-6041-2009, 2009.

Coheur, P.-F., Barret, B., Turquety, S., Hurtmans, D., Hadji-Lazaro, J., and Clerbaux, C.: Retrieval and characterization of ozone vertical profiles from a thermal infrared nadir sounder, J. Geophys. Res., 110, D24303, doi:10.1029/2005JD005845, 2005.

Crutzen, P. J. and Andreae, M. O: Biomass burning in the tropics: impact on atmospheric chemistry and biogeochemical cycles, Science, 250, 1669–1678, 1990.

Duflot, V., Dils, B., Baray, J.-L., De Mazière, M., Atti, J.-L., Vanhaelewyn, G., Senten, C., Vigouroux, C., Clain, G., and Delmas, R.: Analysis of the origin of the distribution of CO in the subtropical southern Indian Ocean in 2007, J. Geophys. Res., 115, D22106, doi:10.1029/2010JD013994, 2010.

AMTD
5, 7567–7586, 2012

Gamache, R. R., Lamouroux, J., Laraia, A. L., Hartmann, J.-M., and Boulet, C.: Semiclassical calculations of half-widths and line shifts for transitions in the 30012 ← 00001 and 30013 ← 00001 bands of CO_2, I: Collisions with N_2, J. Quant. Spectros. Ra., 113, 976–990, 2012.

Hartmann, J.-M., Boulet, C., and Robert, D.: Collisional Effects on Molecular Spectra, Laboratory Experiments and Models, Consequences for Applications, Elsevier Edition, 2008.

Hurtmans, D., Coheur, P.-F., Wespes, C., Clarisse, L., Scharf, O., Clerbaux, C., Hadji-Lazaro, J., George, M., and Turquety, S.: FORLI radiative transfer and retrieval code for IASI, J. Quant. Spectrosc. Ra., 113, 1391–1408, 2012.

Lamouroux, J., Gamache, R. R., Laraia, A. L., Hartmann, J.-M., and Boulet, C.: Semiclassical calculations of half-widths and line shifts for transitions in the 30012 ← 00001 and 30013 ← 00001 bands of CO_2, II: Collisions with O_2 and air, J.f Quant. Spectrosc. Ra., 113, 991–1003, 2012a.

Lamouroux, J., Gamache, R. R., Laraia, A. L., Hartmann, J.-M., and Boulet, C.: Semiclassical calculations of half-widths and line shifts for transitions in the 30012 ← 00001 and 30013 ← 00001 bands of CO_2, III: Self collisions, J. Quant. Spectrosc. Ra., 113, 1536–1546, 2012b.

Li, Q., Jacob, D., Bey, I., Yantosca, R., Zhao, Y., Kondo, Y., and Notholt, J.: Atmospheric hydrogen cyanide (HCN): Biomass burning source, ocean sink?, Geophys. Res. Lett., 27, 357–360, 2000.

Li, Q., Palmer, P. I., Pumphrey, H. C., Bernath, P., and Mahieu, E.: What drives the observed variability of HCN in the troposphere and lower stratosphere?, Atmos. Chem. Phys., 9, 8531–8543, doi:10.5194/acp-9-8531-2009, 2009.

Logan, J. A., Prather, M. J., Wofsy, S. C., and McElroy, M. B.: Tropospheric chemistry: A global perspective, J. Geophys. Res., 86, 7210–7254, 1981.

Lupu, A., Kaminski, J. W., Neary, L., McConnell, J. C., Toyota, K., Rinsland, C. P., Bernath, P. F., Walker, K. A., Boone, C. D., Nagahama, Y., and Suzuki, K.: Hydrogen cyanide in the upper troposphere: GEM-AQ simulation and comparison with ACE-FTS observations, Atmos. Chem. Phys., 9, 4301–4313, doi:10.5194/acp-9-4301-2009, 2009.

Mahieu, E., Duchatelet, P., Bernath, P. F., Boone, C. D., De Mazière, M., Demoulin, P., Rinsland, C. P., Servais, C., and Walker, K. A.: Retrievals of C_2H_2 from high-resolution FTIR solar spectra recorded at the Jungfraujoch station (46.5° N) and comparison with ACE-FTS observations, Geophys. Res. Abstr., 10, EGU2008-A-00000, 2008.

AMTD
5, 7567–7586, 2012

Parker, R. J., Remedios, J. J., Moore, D. P., and Kanawade, V. P.: Acetylene C_2H_2 retrievals from MIPAS data and regions of enhanced upper tropospheric concentrations in August 2003, Atmos. Chem. Phys. Discuss., 10, 29735–29771, doi:10.5194/acpd-10-29735-2010, 2010.

Pumphrey, H. C., Santee, M. L., Livesey, N. J., Schwartz, M. J., and Read, W. G.: Microwave Limb Sounder observations of biomass-burning products from the Australian bush fires of February 2009, Atmos. Chem. Phys. Discuss., 11, 6531–6554, doi:10.5194/acpd-11-6531-2011, 2011.

Rodgers, C. D.: Inverse Methods for Atmospheric Sounding: Theory and Practice, Series on Atmospheric, Oceanic and Planetary Physics, Vol. 2, World Scientific Publishing Co., Singapore, 2000.

Rothman, L. S., Gordon, I. E., Barbe, A., Benner, D. C., Bernath, P. F., Birk, M., Boudon, V., Brown, L. R., Campargue, A., Champion, J.-P., Chance, K., Coudert, L. H., Dana, V., Devi, V. M., Fally, S., Flaud, J.-M., Gamache, R. R., Goldman, A., Jacquemart, D., Kleiner, I., Lacome, N., Lafferty, W. J., Mandin, J.-Y., Massie, S. T., Mikhailenko, S. N., Miller, C. E., Moazzen-Ahmadi, N., Naumenko, O. V., Nikitin, A. V., Orphal, J., Perevalov, V. I., Perrin, A., Predoi-Cross, A., Rinsland, C. P., Rotger, M., Simeckova, M., Smith, M. A. H., Sung, K., Tashkun, S. A., Tennyson, J., Toth, R. A., Vandaele, A. C., and Vander Auwera, J.: The HITRAN 2008 molecular spectroscopic database, J. Quant. Spectrosc. Ra., 110, 533–572, 2009.

Sinha, P., Hobbs, P. V., Yokelson, R. J., Bertschi, I. T., Blake, D. R., Simpson, I. J., Gao, S., Kirchstetter, T. W., and Novakov, T., Emissions of trace gases and particles from savanna fires in southern Africa, J. Geophys. Res., 108, 8487, doi:10.1029/2002JD002325, 2003.

Vigouroux, C., Stavrakou, T., Whaley, C., Dils, B., Duflot, V., Hermans, C., Kumps, N., Metzger, J.-M., Scolas, F., Vanhaelewyn, G., Müller, J.-F., Jones, D. B. A., Li, Q., and De Mazière, M.: FTIR time-series of biomass burning products (HCN, C_2H_6, C_2H_2, CH_3OH, and HCOOH) at Reunion Island (21° S, 55° E) and comparisons with model data, Atmos. Chem. Phys. Discuss., 12, 13733–13786, doi:10.5194/acpd-12-13733-2012, 2012.

Volkamer, R., Ziemann, P. J., and Molina, M. J.: Secondary Organic Aerosol Formation from Acetylene (C_2H_2): seed effect on SOA yields due to organic photochemistry in the aerosol aqueous phase, Atmos. Chem. Phys., 9, 1907–1928, doi:10.5194/acp-9-1907-2009, 2009.

AMTD
5, 7567–7586, 2012

Wiegele, A., Glatthor, N., Höpfner, M., Grabowski, U., Kellmann, S., Linden, A., Stiller, G., and von Clarmann, T.: Global distributions of C_2H_6, C_2H_2, HCN, and PAN retrieved from MIPAS reduced spectral resolution measurements, Atmos. Meas. Tech., 5, 723–734, doi:10.5194/amt-5-723-2012, 2012.

Xiao, Y., Jacob, D. J., and Turquety, S.: Atmospheric acetylene and its relationship with CO as an indicator of air mass age, J. Geophys. Res.-Atmos., 112, D12305, doi:10.1029/2006JD008268, 2007.

Zander, R., Rinsland, C. P., Ehhalt, D. H., Rudolph, J., and Demoulin, P. H.: Vertical column abundance and seasonal cycle of acetylene, C_2H_2, above the Jungfraujoch station, derived from IR solar observations (1991), J. Atmos. Chem., 13, 389–372, 1991.

AMTD
5, 7567–7586, 2012

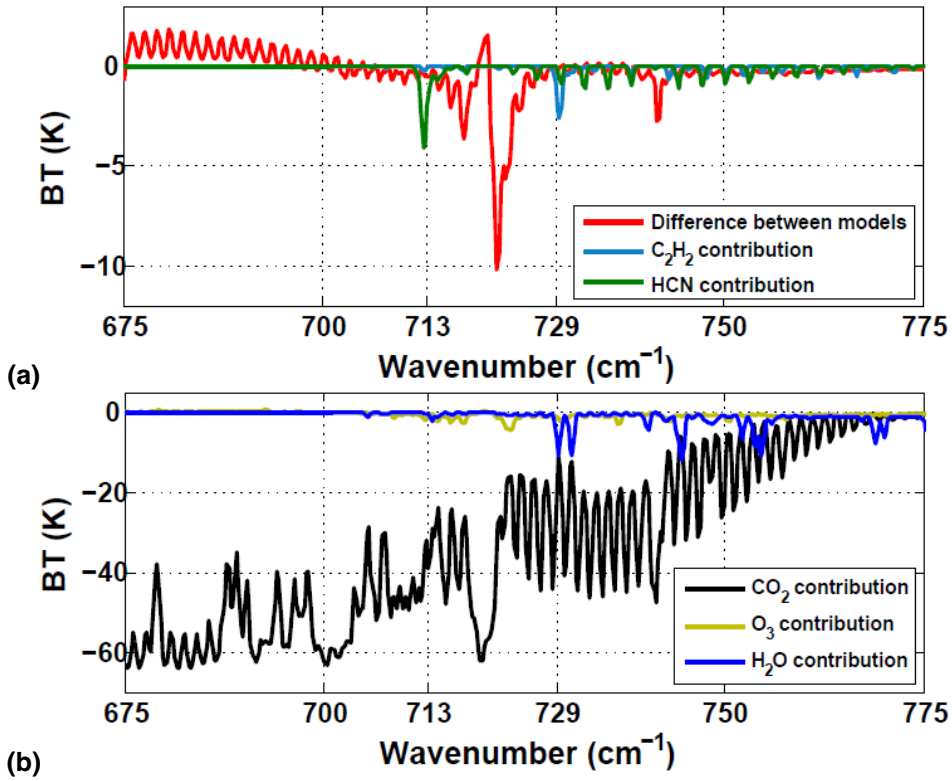

Fig. 1. (a) The red line shows the difference between the forward models with and without CO_2 line mixing considered. To make them visible, contributions of HCN (green line) and C_2H_2 (blue line) are shown for background concentrations multiplied by 40. **(b)**: Contribution of CO_2 (black line), O_3 (ochre line) and H_2O (deep blue line) to a simulated spectrum for background concentrations in a standard atmosphere. Calculations have been made for the US Standard Atmosphere (US Government Printing Office, 1976) with CO_2 concentrations scaled to 390 ppmv.

AMTD
5, 7567–7586, 2012

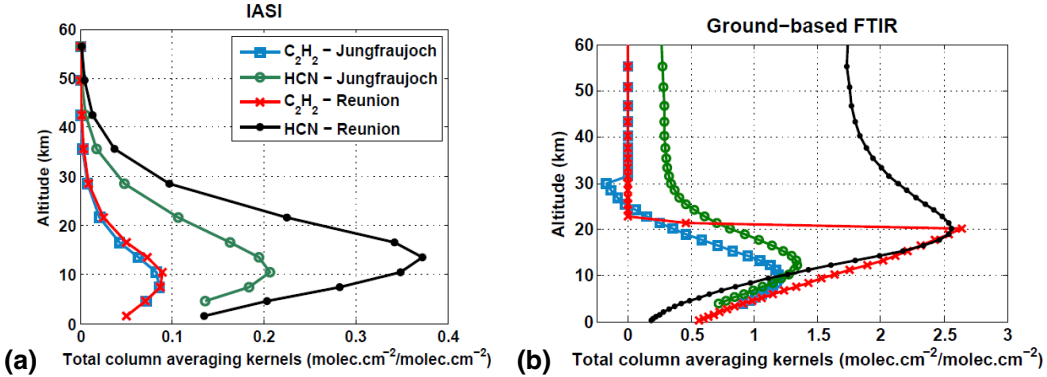

Fig. 2. Total column averaging kernels of IASI **(a)** and ground-based FTIR **(b)** in mol cm^{-2} for C_2H_2 at Jungfraujoch (blue squares and lines), HCN at Jungfraujoch (green circles and lines), C_2H_2 at Reunion (red crosses and lines) and HCN at Reunion (black dots and lines).

AMTD
5, 7567–7586, 2012

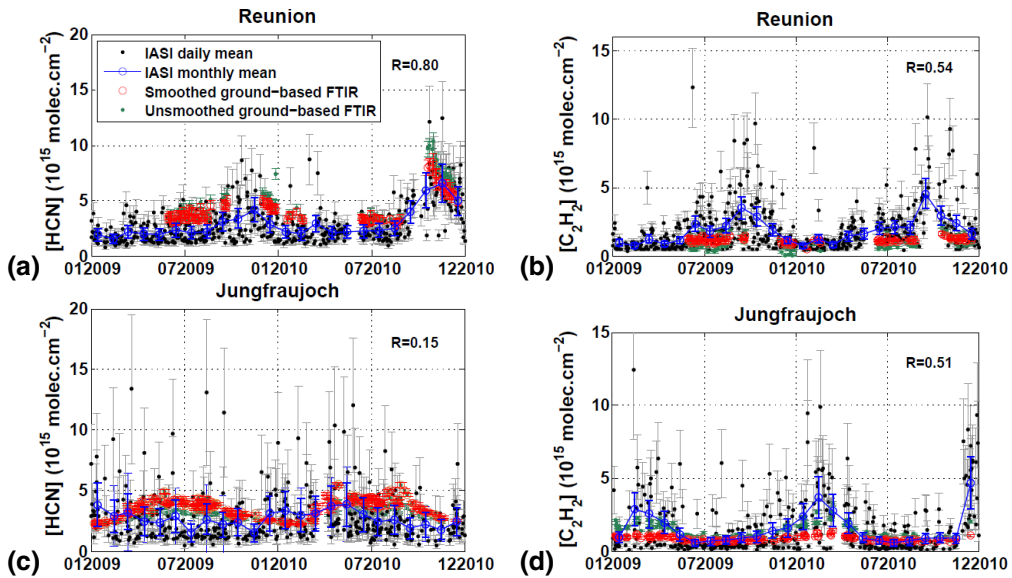

Fig. 3. Time series of HCN and C_2H_2 measurements for Reunion Island (**a** and **b**) and Jungfraujoch (**c** and **d**). IASI measurements are shown as daily and 1° × 1° means (black dots) with associated total retrieval error (gray lines), and as monthly and 1° × 1° means (blue circles and line) with associated total retrieval error (vertical blue lines). Ground-based FTIR measurements smoothed (unsmoothed) with respect to IASI averaging kernels are shown as daily means with associated total error by red circles and line (green dots and line). Correlation coefficients of daily means are given on each plot: **(a)** $R = 0.80$ (101 points), **(b)** $R = 0.54$ (101 points), **(c)** $R = 0.15$ (174 points), **(d)** $R = 0.51$ (174 points).

AMTD
5, 7567–7586, 2012

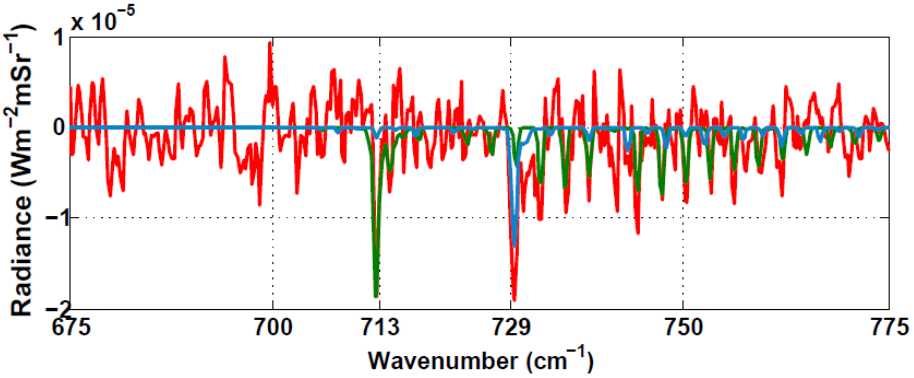

Fig. 4. Difference (red line) between an observed spectrum on 10 October 2010 at 22.35° S and 33.63° E and the corresponding fitted spectrum when HCN and C_2H_2 have been excluded from the fit. The green and blue lines show the contributions at the top of the atmosphere of HCN and C_2H_2, respectively.

AMTD
5, 7567–7586, 2012

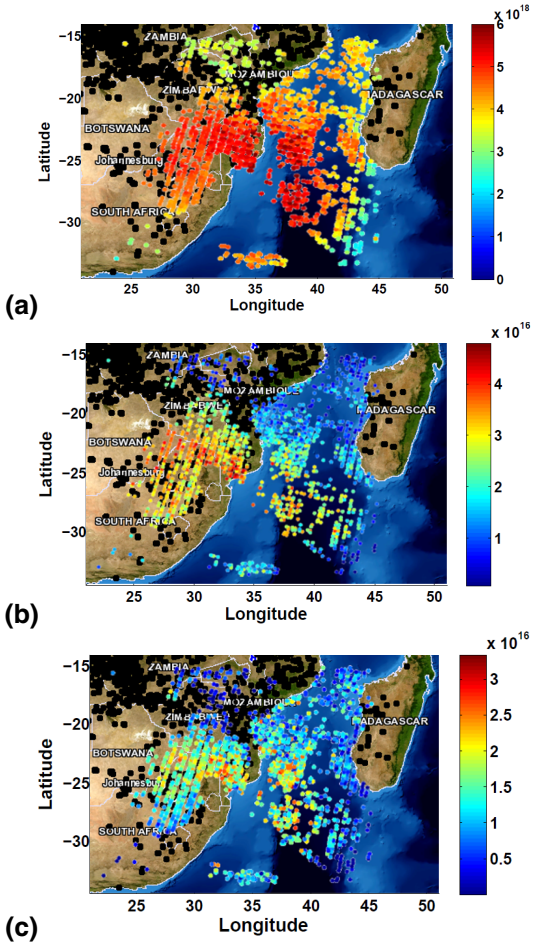

Fig. 5. Total columns of CO **(a)**, HCN **(b)** and C_2H_2 **(c)** on 10 October 2010. Fires spots detected by MODIS on 9 and 10 October are shown by the black dots.

AMTD
5, 7567–7586, 2012

Measurements of hydrogen cyanide (HCN) and acetylene (C_2H_2)

V. Duflot et al.

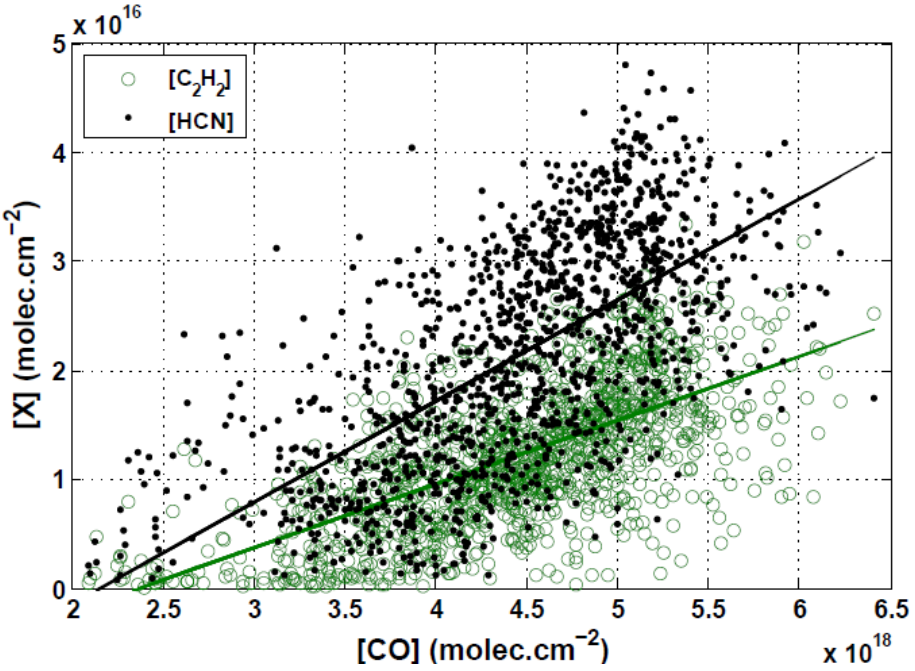

Fig. 6. Correlation plot between CO total columns and HCN (black dots) and C_2H_2 (green circles) total columns for the day and region shown on Fig. 5. The correlation coefficients are 0.72 (1397 points) and 0.68 (1397 points) for HCN and C_2H_2, respectively.

AMTD
5, 7567–7586, 2012